

## Bell-Shaped pH–Rate Profile in a Reaction Involving a Pentacoordinated Phosphorus Intermediate

Andrés Núñez and Oswaldo Núñez\*

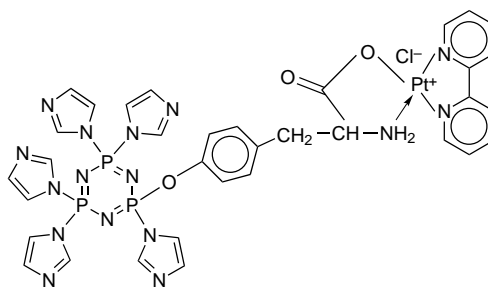
Laboratorio de Fisico-Química Orgánica, Departamento de Procesos y Sistemas,  
Universidad Simón Bolívar, Apartado postal 89000, Caracas, Venezuela

Received April 18, 1996<sup>®</sup>

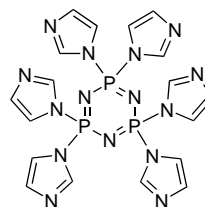
Kinetics of the nucleophilic monosubstitution of imidazole by *p*-nitrophenolate (**PNP**<sup>−</sup>) in hexaimidazolylcyclotriposphazene (**2**) in water: THF 4:1 (5.5 < pH < 7.5) at 24 °C have been studied. The reaction was followed by the disappearance of the **PNP**<sup>−</sup> under pseudo-first-order conditions using the initial-rate procedure. A constant excess of KCl is needed in order to avoid medium effects. A bell-shaped curve is obtained when the  $k_{\text{obs}}$  values (obtained from the leveling or the extrapolation to zero of  $k_{\text{obs}}$  vs  $[\text{H}_2\text{PO}_4^-]_{\text{T}}$  plots) are plotted against the pH. From this plot, a kinetically determined  $\text{p}K_{\text{a}}$  of 5.4 was obtained for **2**. From the same plot, a 5.7 L mol<sup>−1</sup> s<sup>−1</sup> value for the second-order rate constant for the nucleophilic **PNP**<sup>−</sup> attack to the protonated species of **2** was found. A two-step mechanism is proposed. The formed pentacoordinated intermediate cleaves to the (*p*-nitrophenoxy)pentaimidazolylcyclotriposphazene (**3**) in a general-acid-catalyzed reaction. As expected of the proposed mechanism, a change in the rate-limiting step is observed at pH > 7.0 when the  $[\text{buffer}]_{\text{T}}$  increases and  $k_{\text{obs}}$  becomes independent of  $[\text{buffer}]$ . The implications of the present results on the controversial mechanism of hydrolysis of RNA and derivatives are discussed.

### Introduction

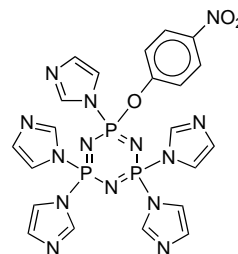
In the search for polyphosphazenes with possible anticancer<sup>1</sup> properties, we have prepared<sup>2</sup> the polymer precursor mono[Pt(bipyridyl)(tyrosil)Cl]penta(imidazolyl)cyclotriposphazene (**1**). Since the capacity of the tyrosine phenol group to displace the imidazole is relevant to the synthesis of **1**, we were interested in studying the removal of the first imidazole group in the hexaimidazolylcyclotriposphazene (**2**) by phenol derivatives. In this paper we present the kinetic results of the displacement of imidazole by *p*-nitrophenolate (**PNP**<sup>−</sup>) in 25% aqueous THF. The kinetics reported were obtained under conditions in which **PNP**<sup>−</sup> is important, thus precluding the mechanistic contribution of the base-catalyzed deprotonation of **PNP**. The advantage of the experimental conditions is that an unambiguous distinction can be made between the anionic attack on the neutral and the protonated state of **2** by kinetics means. In general, this is an important undertaking in reactions involving pentavalent phosphorus intermediates. In addition to contributing to a better understanding of the phosphazene substitution and the direct kinetic measurement of the  $\text{p}K_{\text{a}}$  of **2**, this study may contribute to settling the existing controversy<sup>3–6</sup> on the catalyzed hydrolysis of RNA and derivatives. In fact, some of the manifestations (leveling in plots of  $k_{\text{obs}}$  vs  $[\text{buffer}]$ , bell-shaped pH–rate profiles and strong medium effect dependency) used to argue in favor of or against the unsymmetrical<sup>7</sup> mechanism or the sequential bifunctional-catalyzed mechanism<sup>8</sup> were also present in this study; nevertheless, they are explained without bias by a symmetrical catalyzed mechanism.



1: mono[Pt(bipyridyl)(tyrosil)Cl]penta(imidazolyl)cyclotriposphazene



2: hexaimidazolylcyclotriposphazene



3: (*p*-nitrophenoxy)pentaimidazolylcyclotriposphazene

### Results and Discussion

**Results.** It has been shown<sup>9</sup> that the hydrolysis of **2**, at pH range 6.5–7.8 in 20% aqueous THF, produces hydroxypentaimidazolylcyclotriposphazene. Likewise, the reaction of **PNP** with **2**, under the conditions of this study (pH range 5.4–7.5, water:THF 4:1), produces (*p*-nitrophenoxy)pentaimidazolylcyclotriposphazene (**3**). This

<sup>®</sup> Abstract published in *Advance ACS Abstracts*, November 1, 1996.  
(1) Allcock, H. R.; Allen, R. W.; O'Brien, J. P. *J. Am. Chem. Soc.* **1977**, *99*, 3984.

(2) Angulo, L. M.Sc. Thesis, Universidad Simón Bolívar, 1992.

(3) Breslow, R.; Huang, D.-L. *J. Am. Chem. Soc.* **1990**, *112*, 9621.

(4) Menger, F. M. *J. Org. Chem.* **1991**, *56*, 6251.

(5) Haim, A. *J. Am. Chem. Soc.* **1992**, *114*, 8384.

(6) Breslow, R.; Xu, R. *J. Am. Chem. Soc.* **1993**, *115*, 10705.

(7) Oakenfull, D. G.; Richardson, D. I., Jr.; Usher, D. A. *J. Am. Chem. Soc.* **1967**, *89*, 5491.

(8) Anslyn, E.; Breslow, R. *J. Am. Chem. Soc.* **1989**, *111*, 4473.

(9) Allcock, H. R.; Fuller, T. J. *J. Am. Chem. Soc.* **1981**, *103*, 2251.

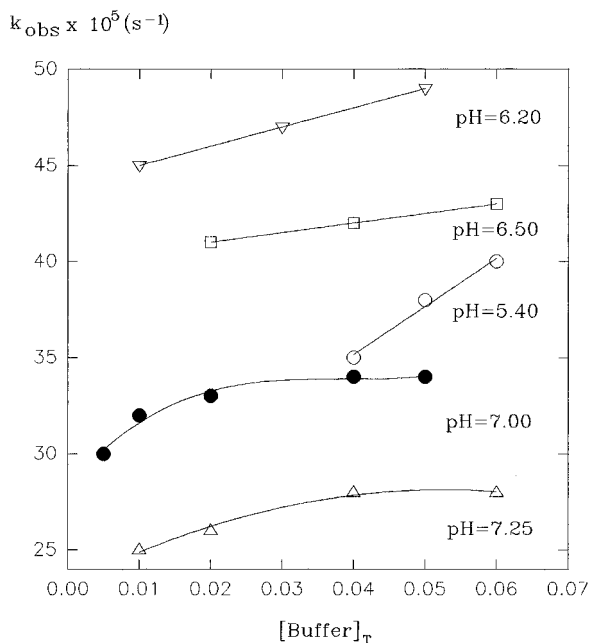


**Figure 1.** Plots of  $k_{\text{obs}}$  (24 °C) vs  $[\text{H}_2\text{PO}_4^-]_{\text{T}}$  at different pH.

reaction was followed under pseudo-first-order conditions by the disappearance of the  $\text{PNP}^-$  absorption at 402 nm or at 320 nm (see Experimental Section). Since the  $[\text{PNP}^-]$  was corrected to the total concentration of  $\text{PNP}$  ( $[\text{PNP}]_{\text{T}}$ ) (see Experimental Section), the rate law is given by

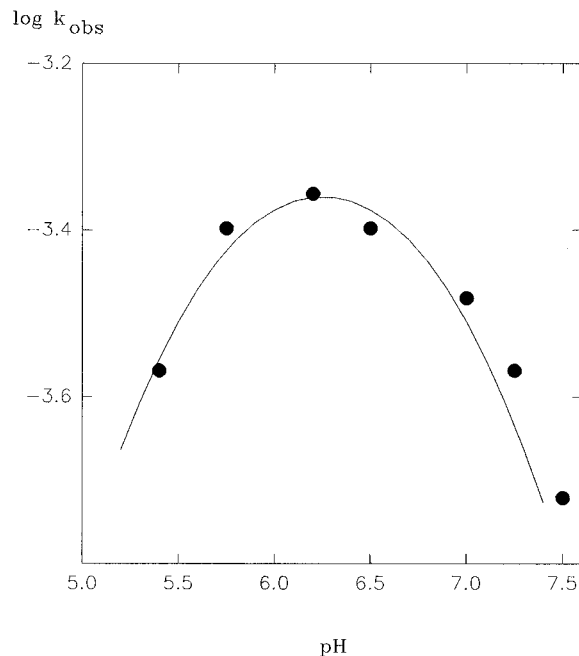
$$-d[\text{PNP}]_{\text{T}}/dt = d[\mathbf{3}]/dt = k_{\text{obs}}[\text{PNP}]_{\text{T}} \quad (1)$$

Figure 1 shows plots of the  $k_{\text{obs}}$  values vs  $[\text{H}_2\text{PO}_4^-]_{\text{T}}$  at different pH. When KCl was not added to the reaction, for instance, at pH = 7.7, an unsymmetrical-bell-shaped  $k_{\text{obs}}$  vs  $[\text{buffer}]_{\text{T}}$  profile (not shown) was obtained, indicating that the reaction rate was extremely sensitive to uncontrolled changes in medium conditions. As shown in Figure 1, the reaction also depends on pH. In fact, when a plot is made of the  $k_{\text{obs}}$  ( $\text{s}^{-1}$ ) with the leveling (general uncatalyzed) lines at pH > 7 and the  $k_{\text{obs}}$  ( $\text{s}^{-1}$ ) obtained from extrapolation to zero buffer concentration (pH < 7) of Figure 1 vs pH, a bell-shaped profile is obtained (Figure 2). The solid line in Figure 2 corresponds to the best-fitting of the experimental points (filled-circles) to the equation

$$k_{\text{obs}} = k_1[\text{H}^+]K'_a[\mathbf{2}]_{\text{T}}/([\text{H}^+] + K_a)([\text{H}^+] + K'_a) \quad (2)$$

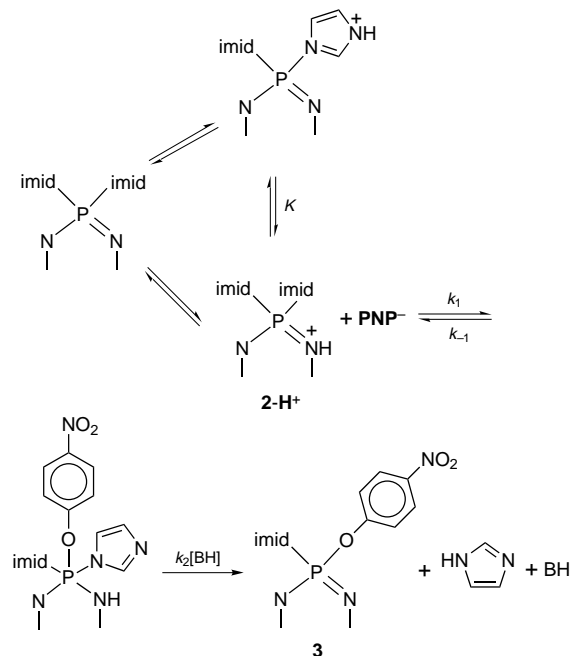
where  $k_1$  (Scheme 1) is the second-order rate constant of nucleophilic attack of  $\text{PNP}^-$  to the  $\mathbf{2}\text{-H}^+$  species,  $[\mathbf{2}]_{\text{T}}$  is the total concentration of  $\mathbf{2}$ , and  $K_a$  and  $K'_a$  are the acidity–equilibrium constants of  $\mathbf{2}\text{-H}^+$  and  $\text{PNP}^-$ , respectively. Since  $K'_a$  is known ( $\text{PNP}$ ,  $\text{p}K'_a = 7.15$ ), a first estimate of the  $k_1$  value ( $2.7 \text{ L mol}^{-1} \text{ s}^{-1}$ ) could be obtained from the  $k_{\text{obs}}$  at pH = 5.4. At this pH, the  $[\text{H}^+]$  is high enough to make the approximation of eq 2 ( $k_{\text{obs}} = k_1[\mathbf{2}]_{\text{T}}K'_a/([\text{H}^+])$ ) valid. Finally, the value of  $K_a$  can readily be obtained by the best fitting to eq 2. The values obtained after the fitting are  $k_1 = 5.7 \text{ L mol}^{-1} \text{ s}^{-1}$  and  $K_a = 10^{-5.4} \pm 10^{-6} \text{ mol L}^{-1}$ .

**Protonation of  $\mathbf{2}$  and  $\text{PNP}^-$  Nucleophilic Attack.** As established by the mechanism of eq 2 (Scheme 1), compound  $\mathbf{2}$  requires protonation before being attacked by the  $\text{PNP}^-$ . This protonation can occur either in the skeleton-nitrogen of  $\mathbf{2}$  or in one of the side-imidazole



**Figure 2.**  $k_{\text{obs}}$  vs pH profile. At pH > 7 the  $k_{\text{obs}}$  were obtained from the non-general-catalyzed (high [buffer]) value of the plots shown in Figure 1. At pH < 7, the  $k_{\text{obs}}$  were obtained from extrapolation to zero [buffer]. The solid line represents the best-fitting of the experimental points (filled circles) to eq 2.

### Scheme 1. Mechanism of Formation of $\mathbf{3}$



substituents. In fact, both alternatives have indicated<sup>10</sup> as possible participants in the hydrolysis mechanism of aminophosphazenes. The  $\text{p}K_a$  of the skeletal nitrogen of  $\mathbf{2}$  is unknown.<sup>9</sup> However, an estimation of this  $\text{p}K_a$  can be obtained using the reported  $\text{p}K_a$  values of hexaamino- and hexaalkoxy-substituted cyclotriphosphazenes. For instance, the  $\text{p}K_a$  in water at 25 °C for the skeleton-nitrogen of hexakis(dimethylamino)cyclotriphosphazene has been reported<sup>11</sup> as 7.45 and as 7.6 in nitrobenzene. Furthermore, the reported<sup>11</sup>  $\text{p}K_a$  value for the hexam-

(10) Allcock, H. R.; Fuller, T. J.; Matsumura, K. *Inorg. Chem.* **1982**, *21*, 515.

ethoxycyclotriphosphazene in nitrobenzene at 25 °C is  $-1.9$ . Although the  $pK_a$  of the imidazolidine is  $14.2^{12}$  and, in principle, its electronegativity capacity could be related to that of an alcohol having a similar  $pK_a$ , such as trifluoroethanol, the real inductive effect exerted by imidazole should be obtained from its inductive contribution ( $\sigma_i$ ). No  $\sigma_i$  value for imidazole has been reported; however, in the case of triazole it has been estimated<sup>13</sup> to be  $0.18$ . If the  $pK_a$  of the hexakis(dimethylamino)-cyclotriphosphazene in nitrobenzene is  $7.6$  with a  $\sigma_i$  value for dimethylamine of  $0.1$ ,<sup>14</sup> and the hexamethoxycyclotriphosphazene has a  $pK_a$  of  $-1.9$  in nitrobenzene with a  $\sigma_i$  of  $0.27$ <sup>14</sup> for the alkoxy group, it is a reasonable assumption that compound **2** with a estimated  $\sigma_i$  value of  $0.18$  for imidazole will have a  $pK_a$  of ca.  $3$ .

The  $pK_a$  for the side-imidazole of compound **2** should be similar to the one found ( $pK_a = 5.38$ ) for the adduct formed by the imidazole attack on the *N,O*-trimethylenephthalimidium cation. This  $pK_a$  value has been obtained<sup>15</sup> from kinetic measurements. Since this protonation necessarily occurs at the distal nitrogen of the imidazole ring, a small variation of this  $pK_a$  value should be expected for the analog protonation of **2**.

As shown in Scheme 1, a fast equilibrium is achieved between compound **2** and its protonated forms. Since the  $pK_a$  of the two protonated forms has been estimated to be ca.  $5.4$  and  $3$  for the side-imidazole and the skeleton-nitrogen, respectively, the equilibrium constant between the two protonated forms can be calculated from the thermodynamic relation  $pK = 5.4 - 3 = 2.4$ . According to the experimental results shown in Figure 2, the  $pK_a$  value obtained for **2** is  $5.4$ . Given the similarities between the measured  $pK_a$  and the  $pK_a$  of the side-imidazole of **2**, one would tend to choose this species as the electrophile that is attacked by the  $\text{PNP}^-$ . However, since the protonation of this species occurs at the distal nitrogen of the imidazole ring, the induced activation of the phosphorus as an electrophile is not as efficient as when the protonation occurs on the nitrogen directly attached to this nuclei. In fact, it has been pointed<sup>15</sup> out that the protonated imidazole is ca.  $10^4$  times slower as a leaving group than expected for an amine of the same  $pK_a$  in which protonation occurs directly on the proximal nitrogen. If this  $10^4$  factor is extrapolated to the activation of phosphorus as an electrophile, it can be established that the side-imidazole-protonated species is at least ca.  $10^4$  times less efficient as an electrophile than the skeleton-nitrogen protonated species. Since the proton transfer between the protonated species of **2** should be fast in comparison with the  $\text{PNP}^-$  nucleophilic attack, the reaction should occur through the less stable protonated species by a factor of ca.  $250$  ( $10^4/10^{2.4}$ ) faster than the more basic imidazole-protonated species. However, the measured  $pK_a$  ( $5.4$ ) is similar to that of the more basic protonated form of **2**. As shown,<sup>16</sup> the measured basicity is largely determined by the strongest basic center. In fact, when the basicity ratio is between the two forms of ca.  $10^2$ , the percentage of protonation of the less basic form is only  $1\%$ . Therefore, the measured

$pK_a$  is mainly determined by the  $pK_a$  of the more basic form of **2**.

#### Cleavage of the Pentacoordinated Intermediate.

According to the mechanism of Scheme 1, once the pentacoordinated intermediate is formed by the  $\text{PNP}^-$  attack on **2-H<sup>+</sup>** (protonated at the skeleton-nitrogen), it cleaves to product **3** via a general-acid-catalyzed mechanism. Since the last protonation now occurs at the distal nitrogen of the imidazole ring ( $pK_a$  ca.  $5$ ), assistance of the buffer should be required for the cleavage of the intermediate in the pH range studied ( $5.4 < \text{pH} < 7.5$ ). As discussed above, a consequence of the protonation at the distal nitrogen of the imidazole ring is that its leaving ability decreases in comparison with that of other protonated amines in which protonation occurs directly in the proximal nitrogen. In fact, the intrinsic leaving ability of the protonated imidazole ring is compared<sup>15</sup> to that of an alcohol of  $pK_a$  ca.  $6$ . Since  $\text{PNP}$  has a  $pK_a = 7.15$ , it is predicted (from ref. 15, Figure 3) that  $\text{PNP}$  will cleave from an intermediate ca.  $10$  times more slowly than the protonated-imidazole. Therefore, it is reasonable that  $k_2[\text{BH}] < k_{-1}$  (second step rate limiting) at low  $[\text{BH}]$  or  $[\text{H}^+]$  and a change in the rate-limiting step of the reaction in Scheme 1 ( $k_2[\text{BH}] > k_{-1}$ ) could be observed, when  $[\text{BH}]$  or  $[\text{H}^+]$  were increased. This is, in fact, the experimental observation in Figure 1 at  $\text{pH} > 7$ . According to the mechanism depicted in Scheme 1, the observed rate-constant is given by the expression

$$k_{\text{obs}} = \frac{k_1[\text{2-H}^+K'_a k_2[\text{BH}]]}{([\text{H}^+] + K'_a)(k_{-1} + k_2[\text{BH}])} \quad (3)$$

When  $k_2[\text{BH}] > k_{-1}$  (first step rate limiting) and when  $[\text{2-H}^+]$  is written as a function of the total concentration of **2**, eq 3 is simplified to eq 2. According to eq 2, the rate should be independent of buffer concentration; however, as shown in Figure 1, the slopes of the straight lines obtained at  $\text{pH} < 7$  are different from zero; therefore, a parallel mechanism where the buffer is present must also be a contributing factor. As can be seen from Figure 1, the slopes increase as the pH decreases; therefore, the parallel mechanism should be one in which the protonated form of the buffer is catalyzing the reaction. The observed rate should therefore be  $k_{\text{obs}} = k_0 + k_2[\text{BH}]$ , where  $k_0$  is given by eq 2 and  $k_2$  is the pseudo-second-order rate constant for the general-acid-catalyzed protonation of **2**. The last constant can be obtained from any of the slopes of the straight lines at  $\text{pH} < 7$ . Since the acidity constant  $K''_a$  of the buffer is known ( $pK''_a = 7.2$ ), the  $k_2$  value can be estimated from the expression  $\text{slope} = k_2[\text{H}^+]/(K''_a + [\text{H}^+])$ . The obtained value is  $0.002 \text{ L mol}^{-1} \text{ s}^{-1}$ .

It is worth mentioning that a distinction between the nucleophilic attack of  $\text{PNP}^-$  on **2-H<sup>+</sup>** and **2** can be achieved from the condition in which the first step is rate-limiting (eq 2). Under these conditions, the attack on the conjugate base **2** will inversely depend on  $[\text{H}^+]$ , and the direct dependency shown (first half of the bell) in Figure 2 will not be observed.

When  $k_2[\text{BH}] < k_{-1}$  (second step rate limiting) and when  $[\text{BH}]$  is written as a function of the total buffer concentration ( $[\text{BH}]_T$ ), eq 3 becomes eq 4. In this equation,  $K_a$  and  $K'_a$  are the equilibrium acidity constants of  $\text{PNP}$  and the buffer ( $\text{H}_2\text{PO}_4^-$ ), respectively. As shown in Figure 1, at  $\text{pH} > 7$  a linear  $[\text{BH}]_T$  dependency is observed at low  $[\text{BH}]_T$  and a leveling is obtained under conditions in which  $k_2[\text{BH}] > k_{-1}$ , where a change in the

(11) Allcock, H. R. *Phosphorus-Nitrogen Compounds Cyclic, Linear and High Polymeric Systems*; Academic Press: New York, 1972; Chapter 12.

(12) Yagil, G. *Tetrahedron* **1967**, *23*, 2855.

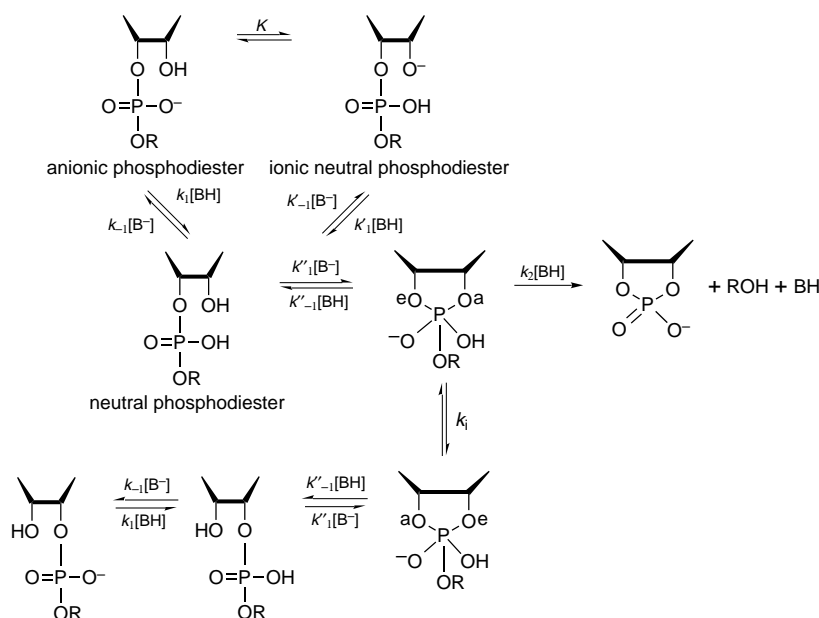
(13) Fox, J. P.; Jencks, W. P. *J. Am. Chem. Soc.* **1974**, *96*, 1436.

(14) Charton, M. *J. Org. Chem.* **1964**, 1222.

(15) Gravitz, N.; Jencks, W. P. *J. Am. Chem. Soc.* **1974**, *96*, 499.

(16) Feakins, D.; Last, W. A.; Nabi, S. N.; Shaw, R. A.; Watson, P. *J. Chem. Soc. A* **1969**, 196.

**Scheme 2. Alternative Mechanism for the General-Catalyzed Hydrolysis at Slightly Acid pH of RNA Derivatives (The Alternative Isomerization Mechanism ( $k_i$ ) Is Also Shown)**



rate-limiting step has occurred and  $k_{obs}$  becomes independent of  $[BH]_T$  as predicted by eq 2.

$$k_{obs} = k_1[2-H^+]k_2K'_a[H^+][BH]_T / k_{-1}([H^+] + K'_a)([H^+] + K'_a) \quad (4)$$

The second step becomes rate limiting ( $k_2[BH] < k_{-1}$  in Scheme 1) only at  $pH > 7$  and at low buffer concentration. This result is a consequence of the special characteristics of imidazole as a leaving group: the intrinsic leaving ability of the protonated imidazole ring is compared<sup>15</sup> to that of an alcohol with a  $pK_a$  of ca. 6, and once protonated it is a ca. 10 times better leaving group than  $PNP^-$  ( $pK_a = 7.15$ ). However protonation of the imidazole ring is required, and its departure becomes slower than that of  $PNP^-$  at low  $[BH]$ .

**Analogy with the Hydrolysis of 3',5'-UpU.** Since a bell-shaped pH-rate profile has also been found<sup>8</sup> in the imidazole-catalyzed hydrolysis of uridylyl(3',5')uridine (**3',5'UpU**), it becomes interesting to explore the possibility that the mechanism proposed for the general catalyzed transformation of **2** to **3** may also be the one operating in the hydrolysis reaction of RNA and derivatives. Accordingly, in the mechanism shown in Scheme 2 the proposed reactive species is either the neutral phosphodiester or the ionic neutral phosphodiester (analog to the intermolecular reaction of  $PNP^-$  and  $2H^+$ ). The equilibrium  $K$  value shown in Scheme 2 is rather unfavorable ( $pK$  ca. 11). This value has been estimated from the thermodynamic relation  $pK = pK_a(2'-OH) - pK_a(POH)$  where  $pK_a$  values of 12.3<sup>17</sup> and 0.7<sup>17</sup> have been found for the 2'-OH and the POH of 3',5'-UpU. Therefore, there is an extremely low concentration of the ionic neutral phosphodiester; however, this unfavorable condition might be balanced by the high reactivity of this species in comparison with the anionic phosphodiester. In fact, it has been found<sup>18</sup> that the neutral species' reaction as an electrophile is ca.  $10^5$  times faster than that of the monoanionic species. Besides, this species is

even more reactive since the nucleophile is  $-O^-$  instead of the  $-OH$  at the attacking group of the monoanionic phosphodiester. In fact the neutral ionic form of phosphodiester has been proposed<sup>17</sup> as the reactive species in the mild acid specific-catalyzed hydrolysis and isomerization of 2',5'- and 3',5'-dinucleoside monophosphates. However, under slightly acidic conditions the most likely general catalyzed path is the one through the neutral phosphodiester in which  $k_{obs}$  is given by the expression

$$k_{obs} = k_1[BH]k'_1[B^-]k_2[BH] / (k'_{-1}[BH]k_{-1}[B^-] + k_2[BH]) \quad (5)$$

Under conditions in which the second step becomes rate limiting ( $k'_{-1}[BH]k_{-1}[B^-] > k_2[BH]$ ) and when  $[BH]$  is written as a total concentration ( $[BH]_T$ ), the  $k_{obs}$  is converted into the expression given by eq 6, where  $K_a$  is the acidity equilibrium constant of the catalyst  $BH$ .

$$k_{obs} = k_1k'_1k_2[BH]_T[H^+] / k'_{-1}k_{-1}([H^+] + K_a) \quad (6)$$

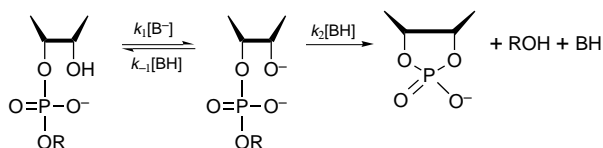
Equation 6 predicts an increase of the  $k_{cat}$  values ( $k_{cat} = k_{obs}/[BH]_T$ ) when pH decreases. Accordingly, it has been reported<sup>8</sup> that in buffer-acetate the isomerization of uridylyl(2',5')uridine (**2',5'UpU**) is catalyzed by the acidic buffer component. The mechanism of Scheme 2 also coincides with the findings<sup>7</sup> in the morpholine-catalyzed ( $pK_a = 8.7$ ) hydrolysis of the phenyl ester of *cis*-tetrahydrofuran-3,4-diol monophosphate, in which the general-catalysis shows a  $k_{cat}$  vs pH profile ( $k_{cat} = k_{obs}/[BH]_T$ ) similar to the one predicted by eq 6. As also shown in Scheme 2, the proposed mechanism for isomerization ( $k_i$ ) becomes independent of buffer concentration. Accordingly, the  $k_{obs}$  vs  $[morpholine]_T$  plots for isomerization<sup>6</sup> of 3',5'-UpU are virtually independent of the morpholine concentration, as expected from the proposed mechanism. Also, the reported<sup>17</sup> results on the specific-catalyzed isomerization of 2',5'- and 3',5'-dinucleoside monophosphates show that  $k_{obs}$  becomes independent on pH.

At higher pH or in the presence of stronger general bases, the ionic neutral phosphodiester should no longer be the reactive species. Instead, the anionic phosphodi-

(17) Järvinen, P.; Oivanen, M.; Lönnberg, H. *J. Org. Chem.* **1991**, *56*, 5396.

(18) Chandler, A. J.; Hollfelder, F.; Kirby, A. J.; O'Carroll, F.; Strömberg, R. *J. Chem. Soc., Perkin Trans. 2* **1994**, 327.

**Scheme 3. Alternative Mechanism for the General-Catalyzed Hydrolysis of RNA Derivatives at Basic pH**



ester will become the active species. However, this latter species requires specific or general base catalyzes due to the low electrophilicity of the phosphorus and the low nucleophilicity of the attacking  $\text{-OH}$  group. Scheme 3 shows a proposed mechanism for general-catalyzed hydrolysis of RNA derivatives at basic pH. According to this mechanism, the observed rate is given by the expression

$$k_{\text{obs}} = k_1 k_2 [\text{B}^-] / (k_{-1} + k_2) \quad (7)$$

In this equation, the base-component of the buffer is the active catalytic species. The experimental results found<sup>6</sup> in the morpholine-catalyzed hydrolysis of **3',5'-UpU** are in agreement with eq 7. In fact, straight lines with slopes that increase along with increases in the base-component fraction are obtained when  $k_{\text{obs}}$  vs  $[\text{morpholine}]_{\text{T}}$  is plotted. When  $[\text{B}^-]$  in eq 7 is written as a function of the total concentration, eq 8 is obtained.

$$k_{\text{obs}} = k_1 k_2 K_{\text{a}} [\text{B}]_{\text{T}} / (k_{-1} + k_2) ([\text{H}^+] + K_{\text{a}}) \quad (8)$$

Therefore,  $k_{\text{cat.}} = k_{\text{obs}}/[\text{B}]_{\text{T}}$  becomes inversely proportional to the  $[\text{H}^+]$  when  $[\text{H}^+] > K_{\text{a}}$  (acidity equilibrium constant of BH) and becomes independent when  $[\text{H}^+] < K_{\text{a}}$ . This  $k_{\text{cat.}}$  vs state of protonation profile has been obtained<sup>8</sup> in the imidazole-catalyzed hydrolysis of **2',5'-UpU**.

### Summary

In summary, a bell-shaped pH–rate profile was obtained in this work in the formation of compound **3** as shown in the mechanism of Scheme 1 and under conditions in which the cleavage of the pentacoordinated intermediate is fast ( $k_2[\text{BH}] > k_{-1}$ ) and eq 2 prevails. According to eq 2, the necessary conditions to obtain a bell-shaped profile are that the  $\text{p}K_{\text{a}}$  of the acid be attacked by the nucleophile having a value similar to that of the buffer (BH) that is being used. This is not the case for the hydrolysis of RNA derivatives, since the  $\text{p}K_{\text{a}}$  of the POH is ca. 1. Therefore, the rate expression for Scheme 2 mechanism (eq 6) does not predict a bell-shaped pH–rate profile, but instead a leveling when the buffer–acid component is increased. However, Schemes 2 and 3 represent an alternative explanation for the general-catalyzed hydrolysis and isomerization of **3',5'-UpU**. As described, in most cases the experimental data obtained fit the corresponding rate expression derived from those equations. Neither the bell-shaped curvature found in the rate vs state of protonation reported in the imidazole-catalyzed hydrolysis of **3',5'-UpU** nor the results obtained from its isomerization can be explained by the mechanism given in Scheme 2. However, it is quite possible that uncontrolled medium effects might be causing

deviation from the predictions. In fact, reactions involving pentacoordinated phosphorus intermediates are very sensitive to medium effects. For instance, a bell-shaped curvature in plots of  $k_{\text{obs}}$  vs  $[\text{buffer}]_{\text{T}}$  was obtained in this work for the formation of **3** when the experiments were done without controlling medium effects. If this is the case, the symmetrical mechanisms shown in Scheme 2 represent quite reasonable alternatives, especially because these proposals are also in agreement with the reported<sup>17</sup> specific-catalyzed mechanism of hydrolysis and isomerization of  $2',5':3',5'$ -dinucleoside monophosphates. The Scheme 3 mechanism has also been proposed lately<sup>19</sup> for the general-catalyzed hydrolysis and isomerization of  $5'$ -*O*-pivaloyluridine  $2'$ - and  $3'$ -(dimethylphosphates), a phosphotriester that mimics<sup>19</sup> the phosphodiester neutral form (methyl ester instead of the oxianion in Scheme 3).

### Experimental Section

**Materials.** Hexachlorocyclotriphosphazene and imidazole were obtained from Aldrich and were used without prior purification; *p*-nitrophenol (spectrophotometric grade) was obtained from Sigma; THF (Aldrich) was distilled from sodium–benzophenone ketyl.

**Synthesis of 2.** Compound **2** was prepared according to the method reported by Alcock and Fuller<sup>9</sup> by slowly adding 0.5 g (1.4 mmol) of hexachlorocyclotriphosphazene in 25 mL of dry THF to a solution of 1.17 g (17.3 mmol) of imidazole in 75 mL of dry THF. The mixture was stirred, at room temperature for 3 h, and filtered (Nitrogen atmosphere) and the solvent volume reduced by one-half. Crystallization was promoted by adding petroleum ether: yield 80%; mp 250–255 °C (lit.<sup>9</sup> mp dec between 254 and 258 °C); NMR (H) ( $\text{CDCl}_3$ )  $\delta$  7.25 (s, 6H), 7.45 (s, 6H), 7.92 (s, 6H). Anal. Calcd for  $\text{C}_{18}\text{H}_{18}\text{N}_{15}\text{P}_3$ : C, 40.07; H, 3.46; N, 39.03; P, 17.32. Found: C, 39.67; H, 3.52; N, 38.20; P, 16.80.

**Buffer Preparation.** Five mL of 2.5 M KCl solution, 5 mL of THF, and the required volume of a 0.5 M solution of  $\text{KH}_2\text{PO}_4$  to obtain a final buffer concentration (25 mL) in the range of 0.005–0.06 M were mixed. Finally, the pH was adjusted to 5.40, 5.75, 6.20, 6.50, 7.00, 7.25, and 7.50 using KOH. Distilled water was added to complete 25 mL.

**Kinetics.** The kinetics reported were obtained under pseudo-first-order conditions at  $5.75 < \text{pH} < 7.50$  by directly following the disappearance of the *p*-nitrophenolate (**PNP**<sup>−</sup>) absorption band (402 nm). The kinetics at pH = 5.40 were followed using the **PNP**<sup>−</sup> absorption band at 320 nm. In all cases the initial-rate method was used. The **PNP** absorbance at each time was transformed to total *p*-nitrophenol concentration using the expression  $[\text{PNP}]_{\text{T}} = A/\Delta\epsilon$ , where  $A$  is the **PNP**<sup>−</sup> absorbance value and  $\Delta\epsilon$  is the slope of a plot of  $A$  vs  $[\text{PNP}]_{\text{T}}$  at each pH. In a typical run, 10 mg of **2** was dissolved in 2.5 mL of buffer solution in a 1 cm UV–vis cell. Ten  $\mu\text{L}$  of **PNP** were added, and the disappearance of the **PNP**<sup>−</sup> absorption band was followed every 30 s during 5 min using a diode arrangement HP-8452A instrument at 24 °C.

The  $k_{\text{obs}}$  were obtained by dividing the slope of a plot of  $[\text{PNP}]_{\text{T}}$  vs  $t$  by  $[\text{PNP}]_{\text{T}}$ . In all the experiments the total concentration of **2** was the same. The final concentrations of each reagent were as follows: **PNP**<sup>−</sup>,  $1 \times 10^{-4}$  M; **2**,  $5 \times 10^{-3}$  M, KCl, 0.6 M; buffer ( $\text{KH}_2\text{PO}_4$ ), 0.005–0.06 M.

**Acknowledgment.** This research was supported by the UGAUSB (Unidad de Gestión Ambiental Universidad Simón Bolívar) and by CONICIT projects S1-2024.

JO9607121

(19) Kosonen, M.; Lönnberg, H. *J. Chem. Soc., Perkin Trans. 2* **1995**, 1203.